Journal of Chemical Reviews, 2020, Volume 2, Issue 4, Pages 228-242

Short Review Article

A Review on Gold Nanoparticles Aggregation and Its Applications

Sakineh Alizadeh [a,b,*], **Zahra Nazari** [b]

[a] *Department of Analytical chemistry, Faculty of Chemistry, Bu-Ali Sina University, 65178638695, Hamadan, Iran*

[b] *Department of Analytical Chemistry, Faculty of Chemistry, Urmia University, Urmia, Iran*

Receive Date: 07 March 2020, **Revise Date:** 18 May 2020, **Accept Date:** 08 June 2020

Abstract:

In recent years, nanoparticles have been classified in three categories namely nanocrystals, films, and quantum dots. Due to the various properties of composites in comparison to individual particles, the studies that are related to the understanding and characterization of these materials have gained much importance. Solvated metal atom dispersion (SMAD) is a technique which includes the vaporization of the metal in a high vacuum reactor and the co-deposition of metallic vapor on the freeze reactor walls at liquid nitrogen temperature. An organic solvent is used to stabilize the metal atoms in the reaction, to form a solvation sphere, before they reach the frozen reactor walls. After the reaction, nanoparticles are warming at room temperature to form metal colloids. In this stage, depending on the metal concentration, metal type, organic solvent and delay time to stabilize the colloidal nanoparticles, the nanoparticles aggregation produce in different shapes (spherical, clusters, and fractals). The SMAD technique due to reducing and stabilizing the metal nanoparticles in a polymer matrix at the time of synthesis, avoiding metal agglomeration and oxidizing of metal nanoparticles does not produce salt. There is great concentration on these compounds as they can be used in medicine as antibacterial coatings, due to the biocidal action of Au nanoparticles (AuNps). Undeniably, numerous selective homogeneous catalysts from nanoparticles have been reported; however, the only feature is the ability of the polymer chain to protect and stabilize the metal particles from oxidation, therefore, the penetration of the reagents for the desired catalytic reactions is possible.

DOI: 10.33945/SAMI/JCR.2020.4.2

Keywords: Aggregation of gold nanoparticles; Nano-biosensor; Dissociation of gold nanoparticles; Laser irradiation; Visual detection; Immunoassay.

Graphical Abstract:

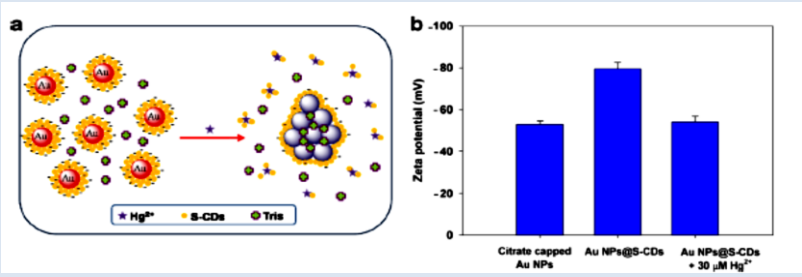

Biography:

Sakineh Alizadeh: In January 2017 Sakineh Alizadeh graduated from the University of Bu- Ali Sina in Hamadan, where she received a bachelor's and master's degree at Shiraz University. Her project on the accumulation of modified nanoparticles for measuring species based on chemometrics tools, the construction of electrochemical nanoscale sensors, Biofuel Cell and the writing of various work and scientific books. At his senior level, she has worked on nano-chemometrics and separation. And now she works as a lecturer at Payam e Noor and Farhangian University.

*Corresponding author: Sakineh Alizadeh, Email: solmaz.alizade@gmail.com

Zahra Nazari: Dr. Zahra Nazari received her bachelor's degree from Arak Azad University. She has a master's degree and a doctorate from Bu Ali University in Hamadan. Her field of work was liquid microextraction at the senior level and her doctoral dissertation on molecular imprinted polymers. She is lecturer of Malayer University.

1. Introduction

The presence of gold nanoparticles in the sub-surface layer of matrix gold grains is extensively common as they are available in weathered rocks of deposits, ore bodies of gold-sulfide and quartz-gold-sulfide formations. Even the probability of their existence is high on the surface of the grains of placer metal in alluvial deposits near the source rocks, though during the transporting process, their surface is subjected to strong mechanical deformations and abrasion. Gold nanoparticles are often seen on the surface of the gold particles in the placers of secondary collectors, and re-deposited weathered rocks [1].

1.2. Ensembles of Micro- and Nanoparticles

Gold nanoparticles normally are found together with the microparticles of noble metal their size is sometimes more than 0.1 lm. The site of the micro and nanoparticles is usually dispersed, but sometimes there are clusters of them. Only particles of nano-sized range can be distributed on the noteworthy areas of the gold surface [1].

1.3. The Morphology of Gold Nanoparticles

It is theoretically demonstrated that the smallest size nanoparticles, including gold, usually have a spherical shape [1]. The reason for this phenomenon is the ample surface energy of the nanoparticles. In addition, electron microscopic study of the gold surface of the numerous gold objects displayed that metal nanoparticles were mainly represented by rounded up to spherical individuals (Figure 1). However, other forms are also available such as worm-like, angular and irregular. Nanoparticles of elongated shape, up to wire-like, were often presented on the surface of gold particles coated with hydroxides of iron (Figure 2).

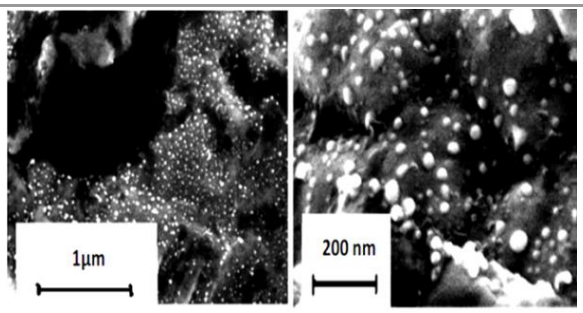

Figure 1. Clusters of gold nanoparticles on the matrix metal surface [1].

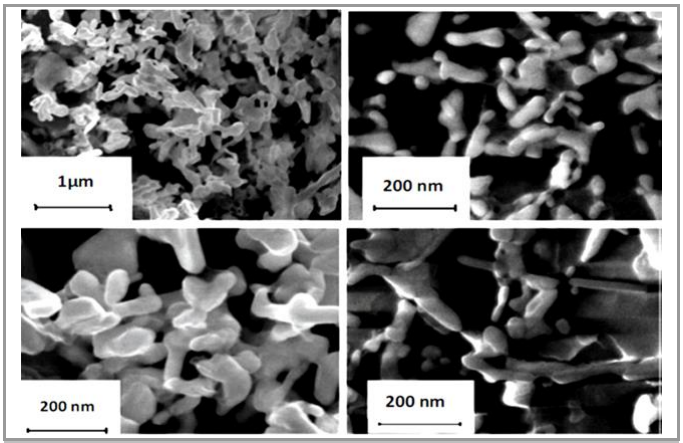

Figure 2. Single and accumulations of gold nanoparticles of elongated shape [1].

In addition to the usual shapes, gold nanoparticles also have hexagonal arrangements. (Figure 3 and 4).

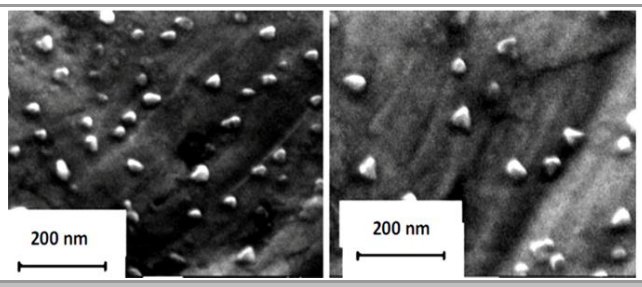

Figure 3. Single and accumulations of gold nanoparticles of elongated shape [1].

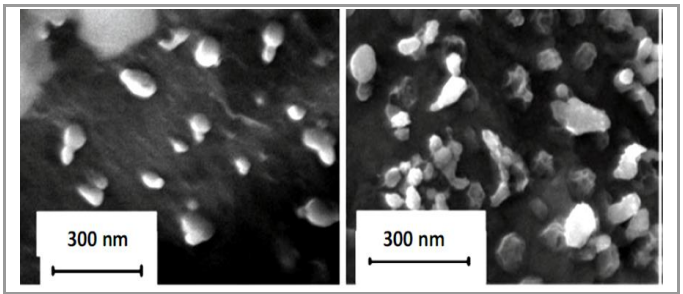

Figure 4. Single and accumulations of gold nanoparticles of elongated shape [1].

The study of the structure of many nanoparticles under high magnification (up to 300–500 thousand times) did not indicate the signs of heterogeneous structure (Figure 5). Also, the complex structure of some nanogold particles, which represent the aggregates of tightly consolidated nanoparticles of different shapes and sizes (Figure 6) [1].

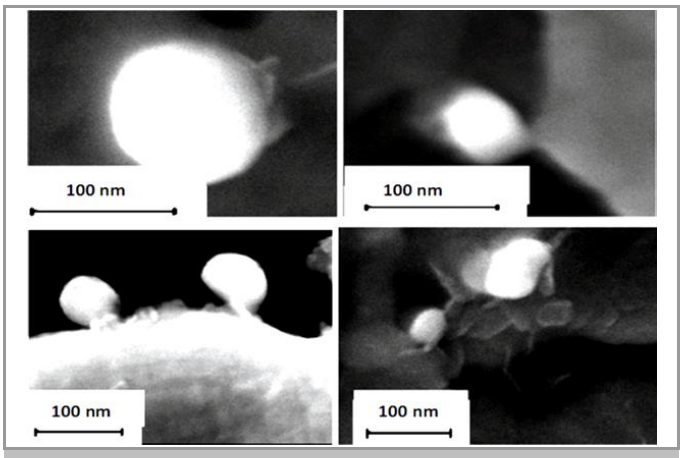

Figure 5. Single and accumulations of gold nanoparticles of elongated shape [1].

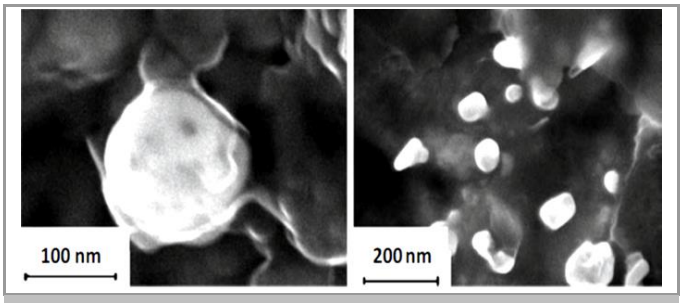

Figure 6. Single and accumulations of gold nanoparticles of elongated shape [1].

1.4. Generations of Nanoparticles

Analysis of electronic microphotographs indicates the possibility of the allocation of single gold nanoparticles in different contacts with the surface of the matrix metal. For instance, some nanoparticles hardly touch the surface of matrix gold, the other have root in a superficial gold layer (Figure 7) [1].

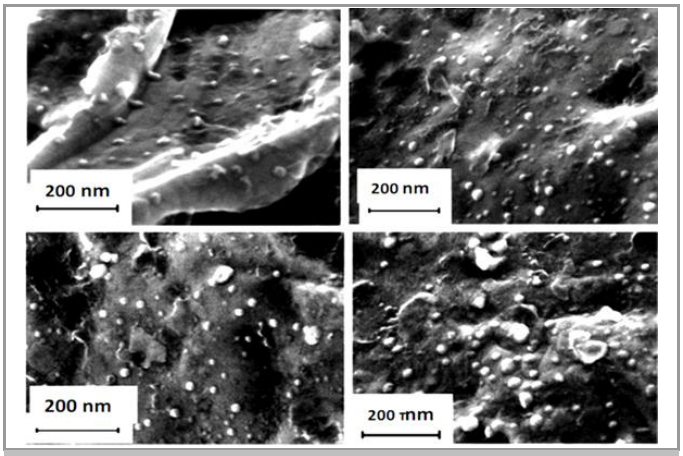

Figure 7. Single and accumulations of gold nanoparticles of elongated shape [1].

This fact indicates the time difference of the deposition of nano-gold on the surface of the matrix gold. In this case probably, individual nanoparticles immerse into the sub-surface layer over time due to the diffusion of metal atoms. It seems that the most "ancient" ones are being completely absorbed in the sub-surface layer.

In this regard, we can distinguish the generations of different age for gold nanoparticles.

The first structures of gold particles were nanoparticles and microparticles, which used microelectronic properties (Figure 8). As a rule, the particle size of the next generation, is smaller than the previous one. These tandems are usually the initial forms that precede the formation of aggregates.

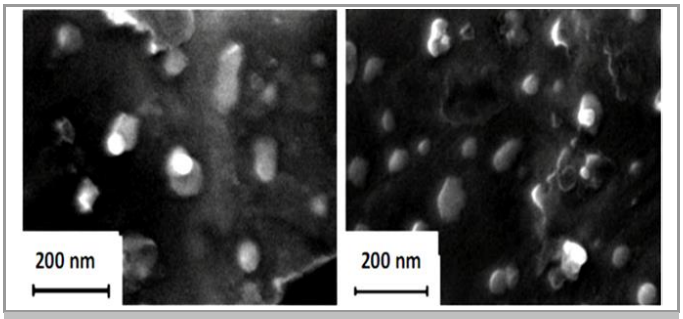

Figure 8. Single and accumulations of gold nanoparticles of elongated shape [1].

Sometimes the morphological features of relatively large rounded gold nanoparticles indicate their concentric zonal structure perhaps, due to layer-by-layer growth of the shell in the range of some core (Figure 9).

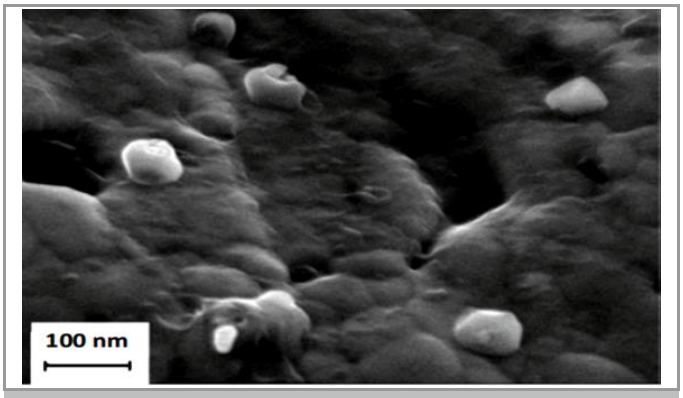

Figure 9. Single and accumulations of gold nanoparticles of elongated shape [1].

2. Gold Nanoparticles in Cancer Treatment

Sztandera *et al*. [4] evaluated the possibility of the use of AuNPs in the treatment of cancer and highlight the recent achievements in this field. All information included here concerns gold nanoparticles, per se, without discussing their complexes in the case of various nanostructures.

Cancer is a general term for a set of genetic diseases characterized by unrestricted, random cell division, and invasiveness. The cancer development is most often caused by mutations or alterations in the expression patterns of protooncogenes, tumor suppressor genes, and those involved in DNA repair. The disruption of pro-apoptotic signaling and overexpression of proteins facilitating cell growth hinder the development of efficient anticancer treatment [4].

Cancer is considered one of the main causes of death worldwide. According to the National Cancer Institute (NCI), there were 14 million new cancer cases and 8.2 million cancer related deaths in 2012. The number of new cases is predicted to increase to 24 million within the next two decades, and about 40% of people may be diagnosed with cancer during their lifetime [4].

In general, nanotechnology is the study of functional systems on a molecular scale. In the context of medicine and biology, nanotechnology includes materials and devices with appropriate structure and function for small sizes, from nanometers (10^{-9} m) to micrometers (10^{-6} m). At this level, the properties of objects are determined just above the scale of a single atom. Thus, nano-size is associated with specific phenomena in both artificial systems and living organisms. The size of nanomaterials is similar to that of essential biological macromolecules and cells.

Therefore, nanomaterials with specific properties can be useful for both in vivo and in vitro biomedical research and applications, actively interacting with cellular components or mimicking various chemical and biological compounds. Combination of nanotechnology and biology may contribute to development of diagnostic devices. Even though the first attempt to apply nanotechnology in medicine was made in the 1960s at ETH Zurich [4], the discoveries from the past few decades revealed new perspectives in the application of nanotechnology in medicine. Currently, scientists can design nanoscale particles (1−100 nm) with defined features (Figures. 10, 11) [4], influencing many fields of science, including chemistry and biotechnology. Due to the highly optimized methods of synthesis, nanoparticles may be featured with monodispersed, diminished cytotoxicity, controllable distribution patterns, and specific mechanisms of interaction with desired ligands. This makes them potentially finest tools for modern medicine. Considering anticancer applications, it is important to note, that nanoparticles have been found to accumulate in tumor tissues through a passive mechanism, known as the enhanced permeability and retention effect (EPR), without the addition of targeting ligands [4]. This is due to the defective tumor vasculature with irregular epithelium, decreased level of lymphatic drainage, and reduced uptake of the interstitial fluid, favoring passive retention of nanoparticles in tumors [4].

Nowadays, there is an increasing interest in nanoparticles of noble metals [4]. The attention of scientists is focused on gold nanoparticles (AuNPs), which have versatile properties and possible applications in clinical chemistry, bioimaging, and therapy of cancer, as well as a targeted drug delivery constantly being characterized.

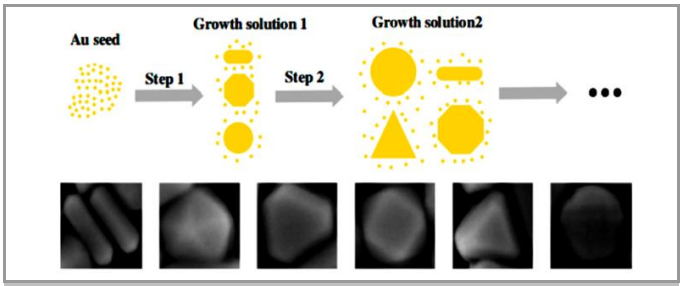

Figure 10. Single and accumulations of gold nanoparticles of elongated shape [1].

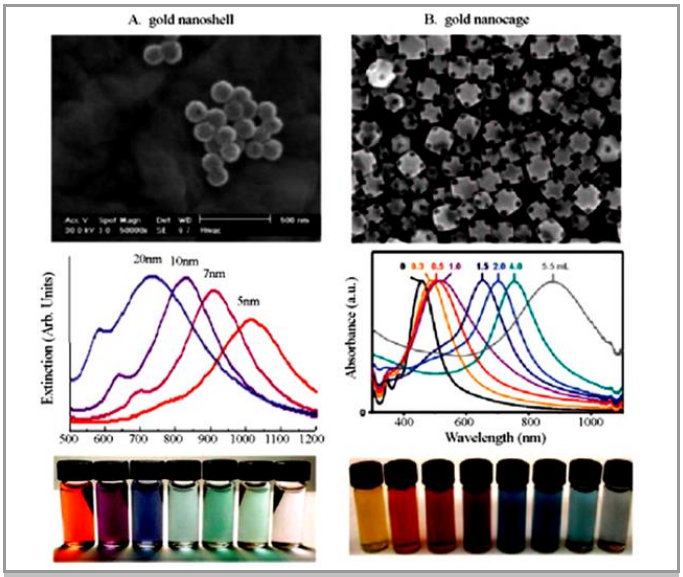

Figure 11. Single and accumulations of gold nanoparticles of elongated shape [1].

The rapid heating of gold nanoparticles causes the formation of vapor bubbles [26], therefore, additional cavitation cell damage upon irradiation occurs with visible [27] or near-infrared light [28]. The capacity of vapor bubble formation has been shown to increase upon the nanoparticle aggregation [29]. Nevertheless, it has to be noted that irradiation of nanoparticles by high-intensity nanosecond IR pulses may cause their rapid destruction, in some cases even after the first dose [30]. On the other hand, the application of femtosecond pulses does not solve this problem since the provided energy is too low. Thus, it is crucial to precisely control the nanoparticles' properties for the particular irradiation strategy. The first study on the possibility to apply gold nanoparticles in photothermal therapy was presented by Hirsch *et al*. in 2003 (Figure 12).

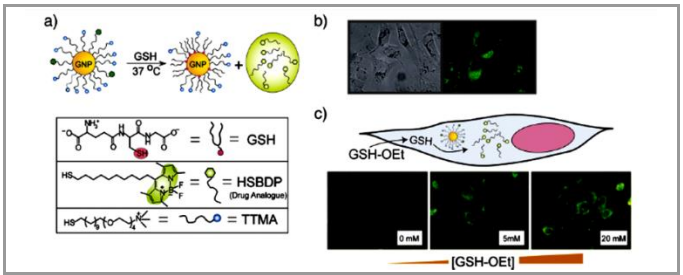

Figure 12. Single and accumulations of gold nanoparticles of elongated shape [1].

3. Ion-Mediated Aggregation of Gold Nanoparticles for Light-Induced Heating

Gold nanoparticles (AuNPs) were synthesized by a modified protocol based on the Turkevich method [32]. A dispersion of citrate-capped spherical gold nanoparticles with a distibution of values of a diameter of 9- 2 nm and a polydispersity index (PDI) of 1.51 was obtained. The polydispersity of the obtained gold nanoparticles was slightly higher than expected from a typical synthesis based on the Turkevich method. We ascribe the higher polydispersity to the presence of impurities in the reaction mixture during the synthesis of the AuNPs. Compared to physical deposition methods, this value of polydispersity is still good. On the other hand, physical deposition methods usually do not suffer from such sensitivity to impurities [32]. Note that our study focuses on the plasmonic features of the gold nanoparticle and its activation through incoming resonant light.

During the synthesis of the nanoparticles, the citrate ions act both as reducing and capping agents. Therefore, the surface of the AuNPs is coated by citrate ions attached by electrostatic and non-specific interactions. The gold nanoparticles display a net negative surface charge at the value of pH of the solution used herein. The AuNPs are thus stabilized by charge repulsion [32].

Therefore, Alba-Molina *et al*., studied the plasmonic photothermal features of the gold nanoparticles under different values of ionic strength by adding sodium chloride to the dispersion of gold nanoparticles. Actually, in our study we did not consider the effect of the so-called "protein corona" formation on the gold nanoparticles [32]. Rather, we seek a fundamental observation on the effect of aggregation on the photothermal capability of the gold nanoparticles against ionic strength (Figure 13).

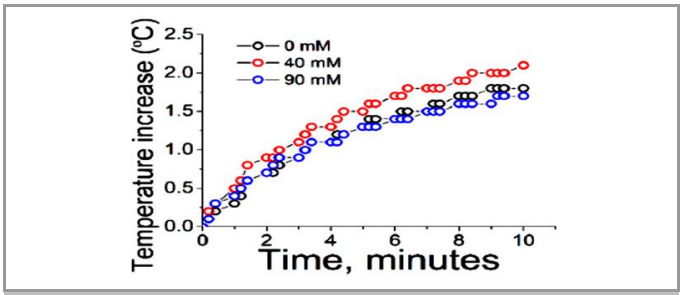

Figure 13. Single and accumulations of gold nanoparticles of elongated shape [1].

4. Chiral recognition in aggregation of gold nanoparticles grafted with helicenes

A chiral organic molecule with two or more chiral centers exhibits stereoisomerism. Since each chiral center has either an R- or S-configuration in central chirality, or a P- or M-configuration in helical chirality, a molecule with n chiral centers can have 2n isomeric forms whose physical, chemical, and biological properties, in principle, are different. Nanoparticles grafted with chiral organic molecules are substances with a number of chiral centers on their surface, where stereoisomerism also occurs. This concept can be used to develop various chiral nanoparticles using a single pair of enantiomeric organic compounds.

In this study, Masahiko Yamaguchi *et al*., synthesized gold nanoparticles grafted with (M)-, (P)-, and (M)-N-(4-mercaptophenyl)-8-methoxycarbonyl-1, 12 dimethylbenzene [c] phenanthrene -5-carboxyamides, which were named P/M-, P-, and M-balls, respectively (Figure 1), and examined their aggregation. It was found that the rate of aggregation was markedly affected by the stereochemistry. A 1: 1 mixture of P-balls and M-balls was less stable in solution towards aggregation than a mixture of P/M-balls, which indicated that the interactions between P- and M-balls were stronger than those between P/M-balls. Since the P-balls/M-balls mixture and P/M-balls contain equal amounts of enantiomeric Helicenes, the chiral recognition phenomena resulted from stereoisomerism. AuNPs with a size distribution of 5–22 nm and a mean diameter of 11 nm were synthesized. Then, one drop of DMF solution containing P/M-balls (5 mg mL_1) was added to aromatic solvents, which exhibited different colors owing to the surface plasmonic bands of gold nanoparticles. The colors were related to the different aggregates formed by nanoparticles, which were studied by UV/Vis and DLS analyses (Figure 14-16) [34].

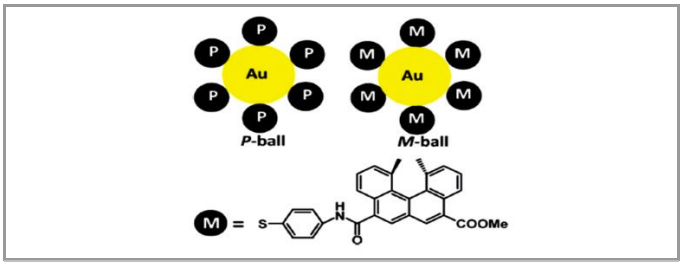

Figure 14. Single and accumulations of gold nanoparticles of elongated shape [1].

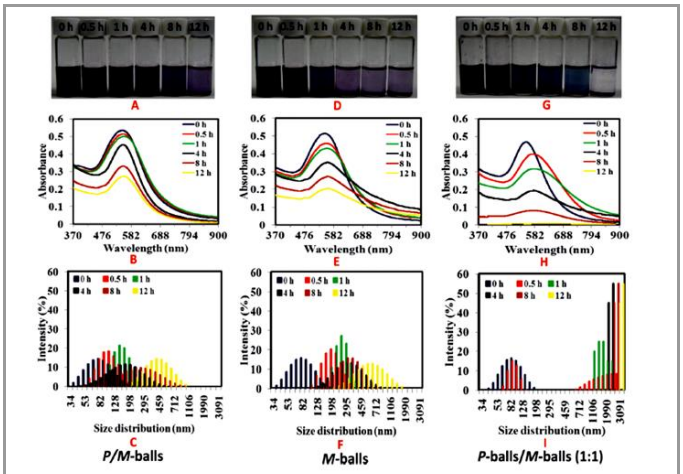

Figure 15. Single and accumulations of gold nanoparticles of elongated shape [1].

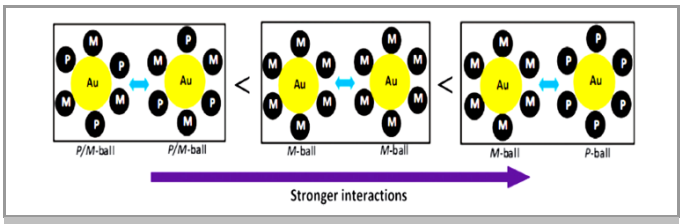

Figure 16. Single and accumulations of gold nanoparticles of elongated shape [1].

5. Detection of Dissolved CO_2 Based on the Aggregation of Gold Nanoparticles

A sensitive colorimetric assay of dissolved CO_2 (dCO_2) was developed based on the plasmon shift of gold nanoparticles (AuNPs). A water-soluble random copolymer poly (dimethyl acrylamideco-(N-amidino) ethyl acrylamide), or P (DMA-co-NAEAA), containing amidine groups was synthesized. At the presence of dCO_2, the amidine groups in the NAEAA block protonate and convert the polymer from a neutral to a positive-charged state, hence triggering the negative-charged AuNPs to aggregate by the electrostatic interaction. The degree of AuNP aggregation is dependent on the charge density of polymer, which is related to dCO_2 concentration [35]. The aggregation of AuNPs results in a red shift of the AuNPs plasmonic spectrum, or a color change from red to blue. In addition, dCO2 concentration can be quantitatively measured by the UV absorbance change of the AuNP solution. A linear relationship between 0.264 and 6.336 hPa of dCO_2 with a limit of detection (LOD) of 0.04 hPa can be acquired. This is the first report to detect dCO_2 using the optical properties of nanoparticles the detection of CO_2, both in gaseous and dissolved phase, plays an important role in environmental monitoring such as in the atmosphere [35-37] in the ocean [38] in rivers and freshwater lakes,[39, 40] and on plants [41]. CO_2 measurements are also important in food and production control [42] in bioreactors [43] in respiration measurement [44] and in blood gas monitoring [45]. Quantification of gaseous CO_2 (gCO_2) level monitoring has been developed by directly measuring the near-infrared (NIR) absorption band of CO_2 between 4200 and 4400 cm^{-1}; however, this method has limited use in detecting dissolved CO_2 (dCO_2) due to the intrinsic IR absorption of water and the complexity of the NIR absorption bands of dCO_2. Currently the main dCO_2 detection methods are potentiometric, solid-state electrolyte, and optical-based methods.

The potentiometric method first was developed by Stow and Randall [46], 60 years ago and subsequently improved by Severing Haus and Bradley [47]. It adopts a CO_2-sensitive glass electrode in a surrounding film of bicarbonate solution covered by a thin plastic membrane permeable to CO_2 but not to water and electrolytic solutes. The CO_2 pressure of a sample gas or liquid equilibrates through the membrane, and the glass electrode measures the resulting pH of the bicarbonate solution. The solid-state electrolyte detection typically relies on charged ion conductance generated at the expense of high-power consumption (300−800 °C), which limits their application in potentially flammable and explosive environments (Figure 17 and 18) [48−50].

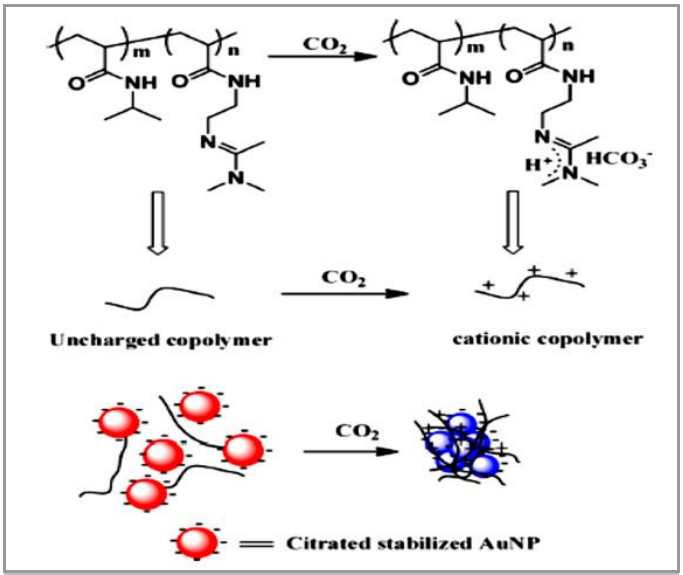

Figure 17. Single and accumulations of gold nanoparticles of elongated shape [1].

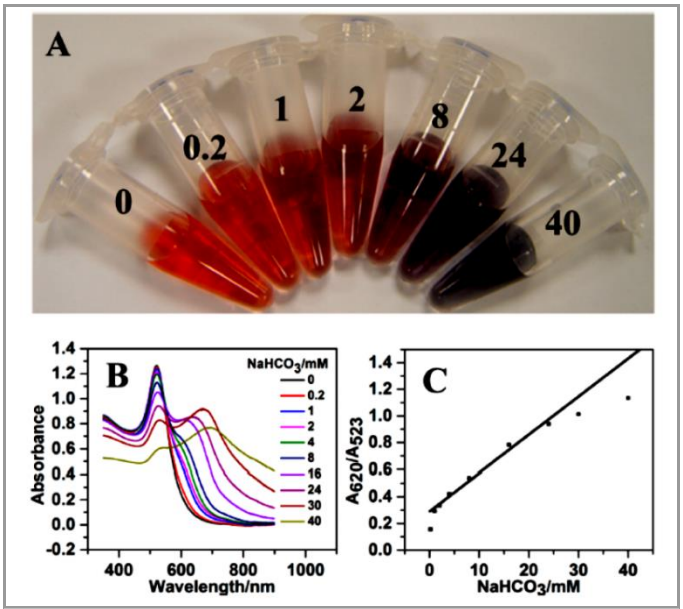

Figure 18. Single and accumulations of gold nanoparticles of elongated shape [1].

6. Rapid Aggregation of Gold Nanoparticles Induced by Non-Cross-Linking DNA Hybridization

In general, a colloidal solution of gold nanoparticles with diameters of 5-20 nm exhibits a red color, because such nanoparticles have an optical absorption peak around 520 nm caused by surface plasmon resonance. Aggregation of the nanoparticles shifts the absorption peak toward longer wavelength and changes the color

of the colloidal solution to purple [2]. Recently, this principle has been applied to analyze various substances such as DNA, lectin, heavy metal ion, potassium ion, and protein. All of these methods are based on the cross-linking mechanism by the target molecules between the gold nanoparticles. For example, Mirkin *et al*. [51] invented a DNA analysis method by modifying two sets of gold nanoparticles with different single-stranded DNA probes and mixed them with target DNA. If the target DNA has sequences complementary to both of the two probes, the target cross-links the nanoparticles by hybridization, and this results in particle aggregation. Detection of a single-base mismatch is possible using this system with appropriate temperature control [51].

On the other hand, aggregation of DNA-functionalized poly (*N*isopropylacrylamide) (PNIPAAm) nanoparticles without the crosslinking mechanism has been reported [11]. In this system, only one kind of single-stranded probe DNA is grafted on PNIPAAm, which spontaneously forms nanoparticles above 40 ºC. When the target DNA is perfectly complementary to the probe, in sequence as well as in chain length the nanoparticles aggregate together at considerably high salt concentration [51].

Although the mechanism of this phenomenon is not fully understood at present, we suppose that conformational transition of the immobilized DNA plays an essential role. Formation of the probe-target duplex makes the conformation tighter and stiffer. This transition may reduce two parts of the repulsive interaction between nanoparticles: (1) electrostatic repulsion may be decreased by the screening effect, because the tight conformation raises the binding constant with counterions [12] and (2) steric repulsion may be reduced, because the stiffening of the DNA lowers the entropic effect [51].

To estimate the number of DNA probes immobilized on the gold nanoparticle surfaces, dithiothreitol was added (final concentration) 10 mM) to release the probes from the nanoparticles into solution [5] Using the OliGreen ssDNA Quantitation Kit (Molecular Probes, Oregon), we measured the concentration of the released DNA to be about 1 M in the stock solution, which means about 200 DNA probes per one nanoparticle (surface coverage) 50 pmol cm^{-2}). This result is comparable to the literature value of 159 DNA probes per one nanoparticle (34 pmol cm^{-2}) [51].

Extinction spectra and particle counting statistics were recorded for the complete set of samples, i.e., for each NP size and the five different immersion times. Measurement of the extinction (absorption plus scattering) spectra is shown in Figure 19. Collective electronic excitations, or surface plasmons, sustained by the metal NPs can be resonantly excited by the incoming optical field at a given wavelength, producing a sharp increment in both the absorption and scattering cross section of the samples, as can be seen in Figure 19 [52].

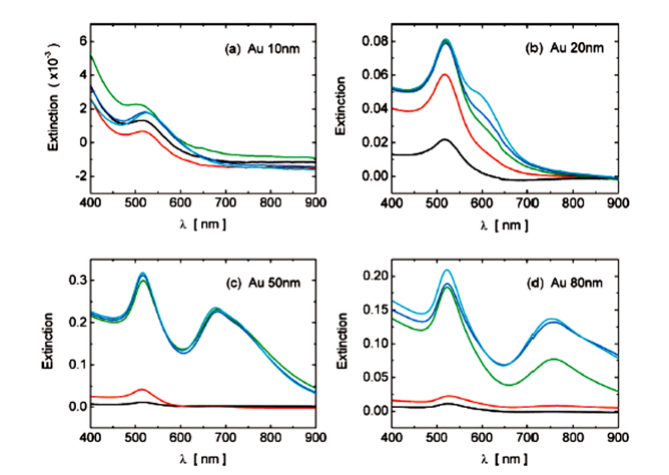

Figure 19. Extinction spectra of APTMS silanized glass substrate, immersed in a solution of AuNPs of (a) 10, (b) 20, (c) 50, and (d) 80 nmin diameter. Black curves correspond to 30 min immersion time, red to 2 h, green to 1 day, blue to 3 days and cyan to 6 days [90].

7. Highly selective aggregation assay for visual detection of mercury ion based on competitive binding of sulfur-doped carbon nanodots to gold nanoparticles and mercury ions

This assay is based on the powerful interaction of Hg^{2+} ion with sulfur atom, the system response toward mercury ion could be affected in the presence of thiolated molecules. The sensitivity was determined by incubation of AuNPs@SC- dots hybrid system with various concentrations of Hg^{2+} with tris and NaCl concentrations fixed at 6 and 3 mM, respectively and the pH value adjusted to 7.5. As expected, after 1 h, the color of solutions changed from red to purple and for higher concentrations of Hg^{2+} to dark blue and gray [53]. This is consistent with the mechanism that higher concentrations of Hg^{2+} displace the carbonic shell more efficiently and AuNPs become less protected against aggregation in tris-NaCl buffered condition. A gradual shift in the SPR band at 520 nm and a new emerged peak at 650 nm demonstrate the contribution of higher concentrations of Hg^{2+} to higher aggregation degree of AuNPs. The ratio of A620/520 was correlated to the concentration of Hg^{2+} and was quantified spectrophotometrically. A linear range of 50 to 1000 nM with the LOD of 47 nM was determined. The LOD was determined by the S/N ratio of 3. Also, another dynamic range for higher mercury ion concentrations (1–4 μM) can be deduced with a smaller slope. The analytical performance of Shamsipur *et al*., colorimetric system has been compared with other AuNPs based probes for mercury ion detection [53].

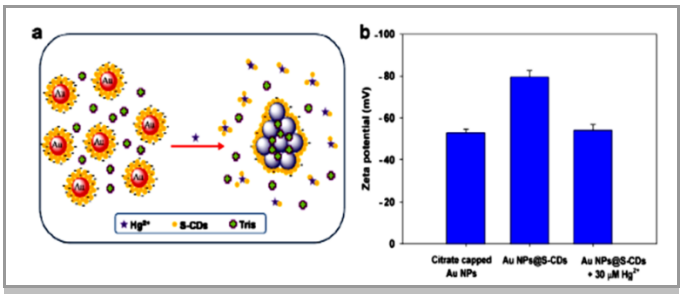

Figure 20. An Hg^{2+} driven displacement of S-C-dots from the surface of AuNPs and subsequent aggregation by tris-NaCl. B Zeta potentials of the citrate-capped AuNPs, AuNPs@S-C-dots nanohybrid, and AuNPs@S-C-dots incubated with 30 μM Hg^{2+}. Error bars represent standard deviations of three measurements (n = 3) [91].

The SPR band of citrate-capped AuNPs shows an absorption band at 520 nm. The decoration of S-C-dots on the surface of AuNPs was simply achieved by hand mixing the aqueous solutions of both nanoparticles. This leads to the formation of a thin layer of carbonic shell around AuNPs without an actual change in the maximum absorption wavelength.

As mentioned earlier, tris-NaCl neutralizes the surface charge of AuNPs by replacing citrate ions on the surface and inducing AuNPs aggregation [53]. Prior to modification of citrate-capped AuNPs with S-C-dots; they readily aggregate in the presence of salts. By modification of AuNPs with S-Cdots and formation of the hybrid nanoparticles, the stability of AuNPs against aggregation increases. The repulsive forces between negatively charged S-C-dots around AuNPs keep them dispersed in the presence of tris-NaCl buffer.

Conjugation of AuNPs with S-C-dots introduces a recognition unit on the surface of AuNPs and allows for colorimetric assaying of Hg^{2+} ions. Incorporation of sulfur atoms into the C-dots structure along with the carboxylic groups on the surface helps S-C-dots to bind mercury ion efficiently. The aggregation of AuNPs is enforced upon addition of mercury ion. Partial displacement of carbonic shell from the nanoparticles (Figure 20) [53] Surface is organized by the high affinity of mercury ion towards S-C-dots. Consequently, the color of solution turns from red to blue. Binding of mercury ion to the free sulfur groups of attached C-dots to AuNPs surface induces color change in the presence of tris-NaCl.

8. Cationic polymers and aptamers mediated aggregation of gold nanoparticles for the colorimetric detection of arsenic (III) in aqueous solution

Yuangen Wu *et. al*. has successfully developed a colorimetric biosensor with high sensitivity and specificity for As (III) detection (Figures 21, 22). The design is based on the aggregation of AuNPs that is controlled by the interaction among PDDA, aptamer and As(III). In the presence of As (III), the aptamer is exhausted firstly due to the formation of an aptamer/As(III) complex, so that the following PDDA aggregates AuNPs, which leads to the remarkable change in color from wine red to blue. Through this approach, As (III) in aqueous solution can be detected as low as 5.3 ppb with high selectivity against other metal ions except for As (V). Such a biosensor owns some advantages. For example, the cationic polymer mediated aggregation of AuNPs is more efficient than other similar sensors, so this sensing method can offer a sensitive and real-time arsenic detection in environmental and other applications. Combined with a portable spectrophotometer, a cost-effective arsenic detection will be realized in the developing countries [54].

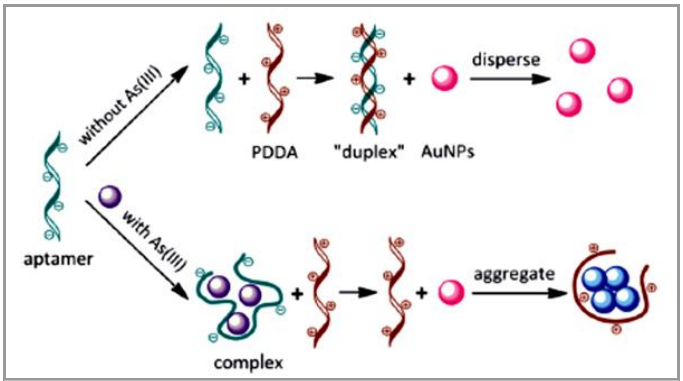

Figure 21. Schematic description of the biosensor for As (III) detection based on the aggregation of AuNPs that is mediated by PDDA and Ars-3 aptamer [54].

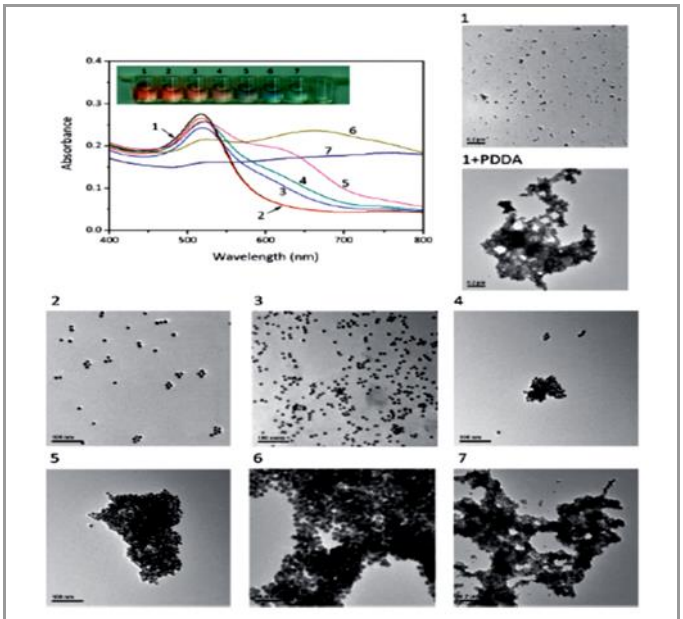

Figure 22. The absorption spectra and transmission electron microscope (TEM) images of the AuNPs solutions treated with different substances. 1: AuNPs; 2: AuNPs + 5 nM aptamer; 3: AuNPs + 5 nM aptamer + 1.52 nM PDDA; 4: sample 3+500 ppb As (III); 5: sample 3+1500 ppb As (III); 6: sample 3 + 2000 ppb As (III); 7: sample 3 + 3000 ppb As (III); Inset: visual color changes of the AuNPs solutions [54].

In the absence of As (III), the Ars-3 aptamers are free and can hybridize with PDDA to form a ‘‘duplex’’ structure, thus the subsequent AuNPs cannot aggregate owing to the lack of PDDA. On adding As(III), the Ars-

3 aptamer is exhausted firstly due to the formation of an aptamer/As(III) complex, so that the subsequent PDDA can aggregate AuNPs, which leads to the remarkable change in color from wine red to blue. The optical property of solution depends on the concentration of PDDA, which is in turn conditioned directly by the content of As(III). Therefore, this strategy makes it possible to detect As (III) by colorimetric assay. It is expected that our method can be also used to detect other metal ions, proteins and small molecules. To confirm the affinity of the Ars-3 aptamer to As (III) and PDDA, circular dichroism (CD) measurement was utilized to monitor the confirmation change of DNA in the system [54].

The aggregation of AuNPs was controlled by the interaction among PDDA, aptamer and As (III). Pure AuNPs dispersed evenly with an average particle diameter of 15 nm (sample 1), and the color of solution was wine red. The introduction of an aptamer did not aggregate AuNPs, but they gathered thoroughly in the presence of PDDA. When PDDA was added into Ars-3 aptamer solution, most of them would exhaust because of the hybridization with DNAs. In this case, the following AuNPs aggregated slightly and caused some increase in absorbance values at 600–650 nm. Subsequently, the biosensor was used to detect As(III), and the results exhibit that AuNPs aggregated gradually, which leads to considerable changes in the color and absorption spectra of solutions[54].

9. Sensitive and selective colorimetric sensing of acetone based on gold nanoparticles capped with L-cysteine

In this work, Bahram *et. Al*. reported that Au nanoparticles (AuNPs) are increasingly utilized as sensitive (bio) chemical probes due to their exceptional physicochemical properties and ease of functionalization. AuNPs, when functionalized with proper ligands, allow the development of highly selective colorimetric sensor. The aim of this paper was to discuss the usage of a reliable and sensitive colorimetric sensor, for sensing dissolved acetone based on the l-cysteine capped gold nanoparticles. The AuNPs were modified with l-cysteine through Au–S bonds. Acetone adsorbs on the surface of l-cysteine AuNPs and induces the aggregation of AuNPs, due to the strong hydrogen-bonds formed between cysteine and acetone. Upon the addition of acetone, the solution showed a color change from red to blue, which was also monitored by visible spectra (Figure 23) [55].

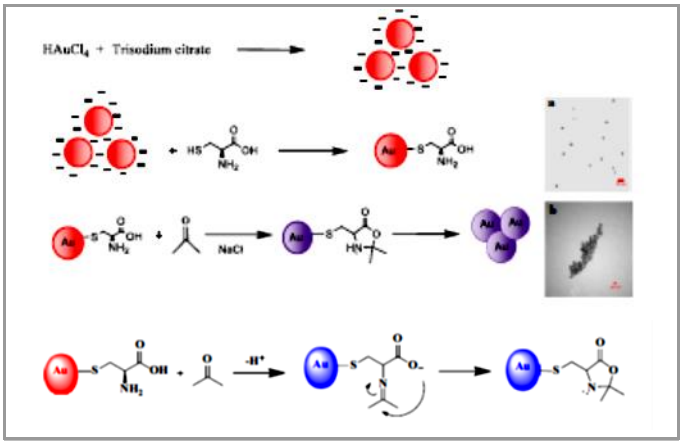

Figure 23. Schematic illustrated aggregation of gold nanoparticles.

10. Colorimetric determination of iodine based on highly selective and sensitive anti-aggregation assay

Iodine as a mineral has great effects on public health; accordingly, there has been an urgent request for iodine selective and sensitive sensor. A colorimetric assay based on the anti-aggregation exclusive feature of gold nanoparticles is presented in this study. The proffered sensor was manufactured in regard to the interaction between thiosulfate and gold nanoparticles, and the forceful inactivation of thiosulfate by iodine. Different concentrations of iodine lead to differential inactivation of thiosulfate, which is in charge of obvious color alteration of AuNPs from blue to red. The quantification of iodine is acquired in relation to the alteration in the surface plasmon resonance absorption of the gold nanoparticles. Under the optimum condition, the limit of detection is 1.36 nmol L^{-1} with the linear range from 3 to 80 nmol L^{-1}. Further utilization of the proposed colorimetric method to determine iodine in human serum presented satisfying consequence concerning selectivity and sensitivity (Bahram *et. Al*.) (Figure 24) [56].

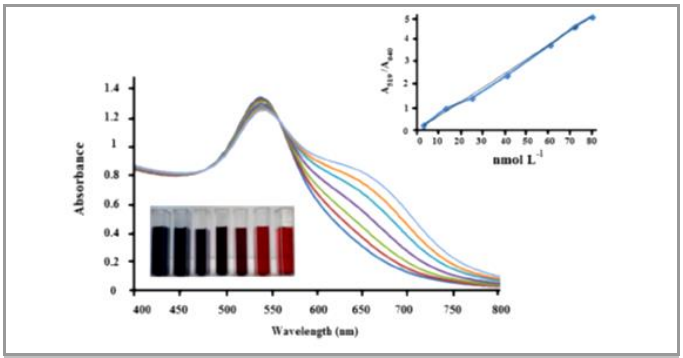

Figure 24. UV–Vis spectra and images of AuNPs in the presence of 5.94 mmol L^{-1} thiosulfate with various concentrations of iodine and calibration curve of A_{519}/A_{640} versus iodine concentrations; under optimum conditions in the range of 3–80 nmol L^{-1}.

11. Gold nanoparticles bio-functionalized (grafted) with chiral amino acid: a practical approach to

determining the enantiomeric percentage of the racemic mixtures

The importance of stereochemistry in chiral drugs is due to the different pharmacological behavior of enantiomers. Enantioseparation methods based on nanoparticles have gained interest recently. The different interaction of enantiomers with chiral 10 nanoparticles encouraged us to determine the enantiomeric percentage of racemic mixtures with modified gold nanoparticles. In this work we applied L-Cysteine capped gold nanoparticles (chiral environment) as a colorimetric sensor for enantio-selective detection of naproxen (NAP) racemic mixtures. The selective and rapid aggregation of modified gold nanoparticles in the presence of R-naproxen allowed us to construct a visual chiral sensor. The effect can be monitored with naked eye or using a UV-vis spectrometer. The developed method was utilized for the determination of enantiomeric percentage of the racemic mixtures of NAP in aqueous and plasma samples with satisfactory results (Figure 25) [56].

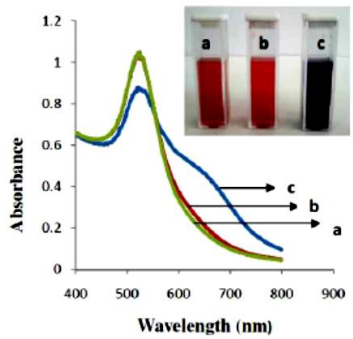

Figure 25. UV-vis absorption spectra of (a) L-cysteine capped Au NPs (b) L-cysteine capped Au NPs response to S-naproxen (c) L-cysteine capped Au NPs response to R-naproxen.

12. Highly selective and sensitive determination of dopamine in biological samples *via* tuning the particle size of label-free gold nanoparticles

Mohseni *et al*., reported a rapid, sensitive and selective approach for the colorimetric detection of dopamine (DA) was developed utilizing unmodified gold nanoparticles (AuNPs). This assay relied upon the size-dependent aggregation behavior of DA and three others structurally similar catecholamines (CAs), offering highly specific and accurate detection of DA. By means of this study, we attempted to overcome the tedious procedures of surface premodifications and achieve selectivity through tuning the particle size of AuNPs. DA could induce the aggregation of the AuNPs via hydrogen-bonding interactions, resulting in a color change from pink to blue which can be monitored by spectrophotometry or even the naked-eye (Figure 26) [57].

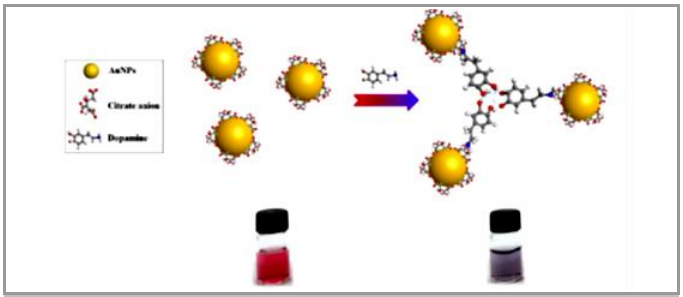

Figure 26. Schematic illustration of possible interaction mechanism of citrate-capped AuNPs and DA (gray: C; blue: N; red: O; white: H).

13. Chemical Nose for Discrimination of Opioids Based on Unmodified Gold Nanoparticles

Bahram *et al*., reported a colorimetric sensor array based on unmodified gold nanoparticles (AuNPs) for the first time in order to sensitively detect and identify multiple structurally similar opioids including morphine, codeine, oxycodone, noroxycodone, thebaine, tramadol and methadone in aqueous media. Size dependency of assembly process encouraged us to employ AuNPs with four distinct particle sizes as sensing elements and visual differentiation tools to construct a colorimetric nanoarray. The target opioids seem to act as "molecular bridges", shortening the interparticle distance and inducing the aggregation of AuNPs. This aggregation produces changes in both the color and UV-vis spectra of AuNPs generating a visual molecular fingerprint of each analyte [58]. The cumulative array responses were differentiated by principal component analysis (PCA) and hierarchical cluster analysis (HCA) with 100% classification accuracy demonstrating the versatility of this simple nanoarray platform. Furthermore, color difference maps were created to provide a visual tool for classifications and semi-quantitative analysis without exploiting any statistical techniques. Finally, we demonstrated the ability of the constructed array to identify the various opioids in urine sample. The obtained results suggest that the proposed colorimetric nanoarray has promising perspective in the clinical toxicology and forensic cases for the on-spot detection of illegal drugs (Figure 27) [59].

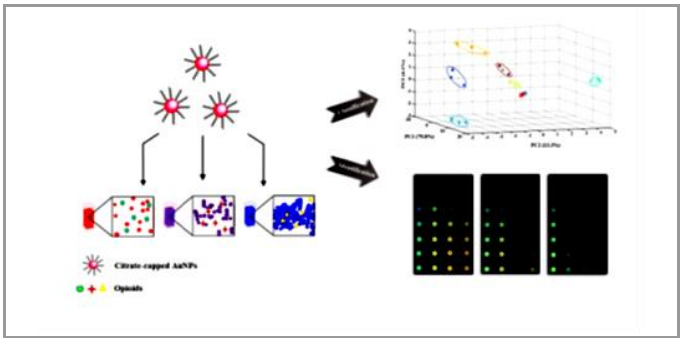

Figure 27. Schematic illustrated Chemical Nose for Discrimination of Opioids Based on Unmodified Gold Nanoparticles.

14. Application of Silver Nanoparticles for Simple and Rapid Spectrophotometric Determination of Acetaminophen and Gentamicin in Real Samples

Silver nanoparticles (AgNPs) have been widely rummaging during the past decades due to their interesting optical and electric properties and potential applications in catalysis, electronics, bio-labelling, surface-enhanced Raman scattering (SERS), etc. Spectrofluorometric and spectrophotometric nanoparticles have received much attention in analytical chemistry because of their unique properties originating from the quantum size effect. They are obviously different from those of the corresponding bulk materials in terms of sensitivity. The optical properties of metal nanoparticles are highly affected by the preparation methods and conditions, which result in particles of various sizes; shape and surface stabilization. Moreover, the surface/interface interactions have their signatures in the properties investigated. In this work, Madrakian *et al*., explained the application of silver nanoparticles (AgNPs) for spectrophotometric determination of acetaminophen (AC) and gentamicin (GEN) (Figure 28) [60].

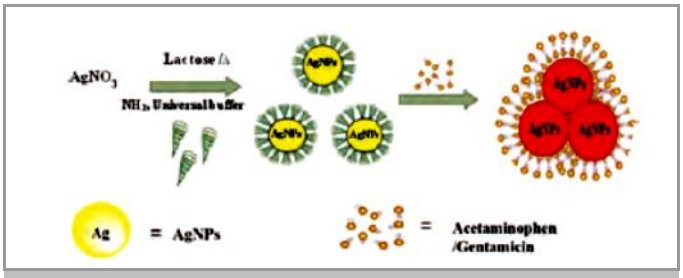

Figure 28. Aggregation of silver nanoparticles.

15. Highly Selective and Sensitive Simultaneous Determination of Hemoglobin and Folic Acid Based on the Aggregation of PHCA Modified-Gold Nanoparticles Using Partial Least Square

In this study Alizadeh *et al*., describe a spectrometric monitored kinetic process for highly selective and sensitive simultaneous determination of hemoglobin (Hem) and folic acid (FA) based on the aggregation of gold nanoparticles (Au NPs) modified with N,N-biphenyl hydrazine 1,2 carbothioamide (PHCA). The method is based on the differences of aggregation rates of modified Au NPs in the presence of hemoglobin (Hem) and folic acid. Kinetic-spectrophotometric profile of aggregation processes were recorded in aqueous media at pH 6 (phosphate buffer). Subsequently, partial least square (PLS) modeling is carried out for analyzing the obtained data. The sensitivity and selectivity of Au NPs toward other drugs as potential interferents were also studied (Figure 29) [61].

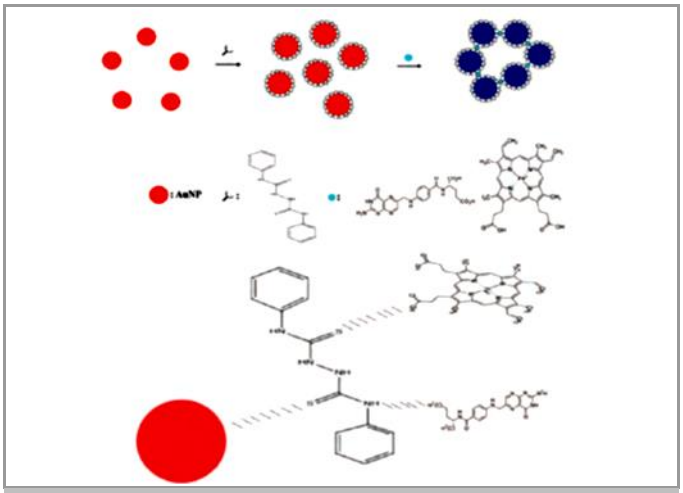

Figure 29. Schematic for possible interaction and possible mechanism of PHCA to AuNPs and Hem/FA to PHCA@AuNPs.

16. Simple and rapid Simultaneously Colorimetric determination of betamethasone and nephazoline based on partial least square using gold nanoparticle probe

Gold nanoparticles (Au NPs) have attracted enormous scientific and technological interest due to their ease of synthesis, chemical stability, and unique optical properties. In this work Alizadeh *et al*., reported that the absorbance of the Au NPs at 520 nm decreased and in 640 increased with the increase in the concentration of betamethasone (BET) and nephazoline (NEP). The rate of absorbance change in these drugs is difference. For this reason, we can simultaneously determine the BET and NEP. The color change of the Au NPs with different concentrations of these drugs could make it convenient to be observed by the naked eye. The formation of Au NPs in the presence of citrate was monitored by transmission electron microscopy (TEM) and UV-Vis spectroscopy. The experimental conditions were optimized to obtain the highest yield for nanoparticle formation. Partial least square (PLS) regression as an efficient multivariate spectral calibration method was employed to make a connection between the SPR spectra of the generated Au NPs. The number of PLS latent variables was optimized by leave-one-out cross-validation utilizing prediction residual error sum of square (PRESS) (Figure 30) [62].

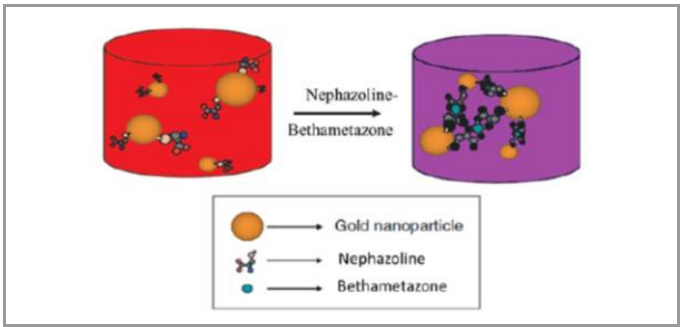

Figure 30. Schematic illustrated Colorimetric determination of betamethasone and nephazoline based on partial least square using gold nanoparticle probe

17. Simultaneous colorimetric determination of morphine and ibuprofen based on the aggregation of gold nanoparticles using partial least square

In this work Bahram etal reported a new method for simultaneous colorimetric determination of morphine (MOR) and ibuprofen (IBU) based on the aggregation of citrate-capped gold nanoparticles (AuNPs). Citrate-capped AuNPs were aggregated in the presence of MOR and IBU. The difference in kinetics of AuNPs aggregation in the presence of MOR/IBU was used for simultaneous analysis of MOR and IBU. The formation and size of synthesized AuNPs and the aggregated forms were monitored by infra-red (IR) spectroscopy and transmission electron microscopy (TEM), respectively. By adding MOR or IBU the absorbance was decreased at 520 nm and increased at 620 nm. The difference in kinetic profiles of aggregation was applied for simultaneous analysis of MOR and IBU using partial least square (PLS) regression as an efficient multivariate calibration method. The number of PLS latent variables was optimized by leave-one-out cross-validation method using predicted residual error sum of square. The proposed model exhibited a high capability in simultaneous prediction of MOR and IBU concentrations in real samples (Figure 31) [63].

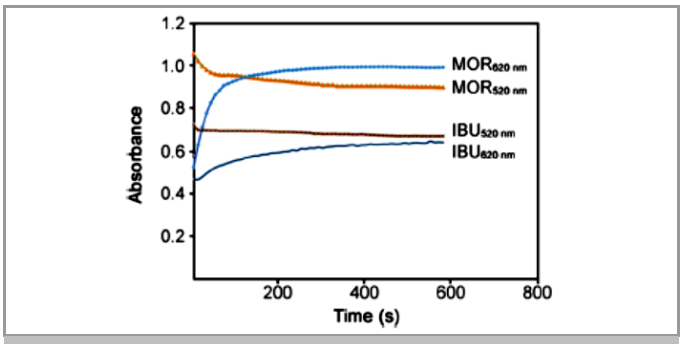

Figure 31. Change in absorbance of AuNPs at 520 and 620 nm versus time (kinetic profiles) by injection of morphine and ibuprofen. Conditions: morphine/ibuprofen concentration 5.0 µg/mL, temperature 25 °C, ionic strength 1 mmol/L, pH 6, AuNPs 10 nmol/L..

18. Rank Annihilation Factor Analysis for Spectrophotometric Study of Morphine Based on Gold Nanoparticle Aggregation Using Multivariate Curve Resolution

Alizadeh *et al*., reported the use of rank annihilation factor analysis (RAFA) for spectrophotometric studies in one-step aggregation of gold nanoparticles processes. When the aggregation process constant acts as an optimizing object, and simply combined with the pure spectrum of gold nanoparticles, the rank of original data matrix can be reduced by annihilating the information of the gold nanoparticles from the original data matrix. The residual standard deviation (R.S.D.) of the residual matrix after bilinearization of the background matrix is regarded as the evaluation function. For aggregation process, the effects of noise level and equilibrium constants K on output of algorithm were investigated. Also, multivariate curve resolution was used for derived spectra, loading and score. For prediction of aggregation rate constant solver program was also used (Figure 32) [64].

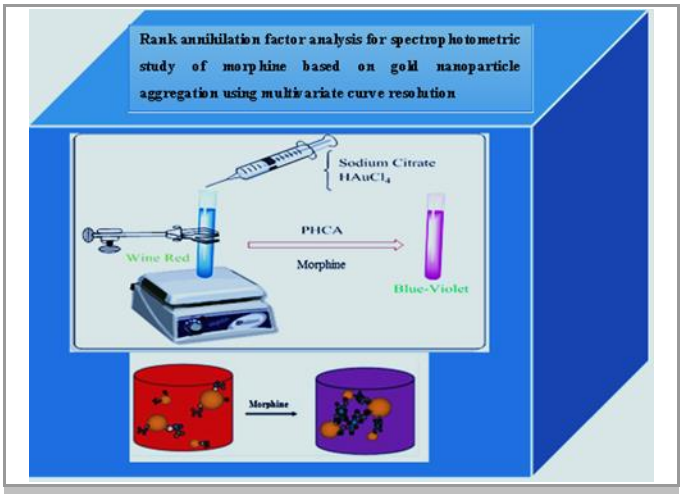

Figure 32. Schematic illustrated Factor Analysis for Spectrophotometric Study of Morphine Based on Gold Nanoparticle Aggregation.

19. Conclusion

This work discussed the identification and discrimination of opioids in aqueous solution based on the modified AuNPs as sensing elements. The proposed colorimetric sensor array without the necessity of the complicated procedures offers a convenient platform for visual differentiation of elements. We believe that this straightforward NPs-based detection system by making some improvements can be easily adopted to differentiate other groups of analytes and biological targets for which the development of highly specific sensors is challenging. The SPR of the AuNPs, synthesized by reduction of gold ion with citrate, were used as a novel analytical method for determination of drugs and species based on aggregation of these nanoparticles. A direct relationship was found between the levels of drugs and difference in intensity of AuNPs spectra with time in λmax at about 520 and 640 nm. In comparison with the available analytical methods for simultaneous determination of species, the proposed method has the following advantages: (i) it needs lower amounts of reagents; (ii) since this method is selective, the method in real samples can be determined without any initial sample preparation. (iii) The proposed method has a simple, fast, and low cost procedure, in contrast to chromatographic methods, this method does not need any expensive apparatus, and (iv) compared with spectrophotometry combined with chemo metrics, both methods similarly need the minimum sample preparation steps and one cannot prefer one over another for sample preparation complexity. A visible color change of AuNPs from wine red to blue was evident by naked eye. The developed method was

found to be very sensitive and simple without any further modification of AuNPs.

Acknowledgment

The authors acknowledge the Bu-Ali Sina University Research Council and Center of Excellence in Development of Environmentally Friendly Methods for Chemical Synthesis (CEDEFMCS) for providing support to this work.

Disclosure statement

No potential conflict of interest was reported by the authors.

References

[1] B. Osovetsky, Natural Nanogold, Nanomineralogy Sector, Mineralogy and Petrography Department, Perm State National Research University, Perm, Russia, Springer Mineralogy, **2017**, 11-40.

[2] Alizadeh, S., Madrakian, T., & Bahram, M. (**2019**). Selective and Sensitive Simultaneous Determination of Mercury and Cadmium based on the Aggregation of PHCA Modified-AuNPs in West Azerbaijan Regional Waters. *Advanced Journal of Chemistry, Section A: Theoretical, Engineering and Applied Chemistry*, *2*(1), 57-72.

[3] Kyzas, G. Z., Bikiaris, D. N., & Lazaridis, N. K. (**2008**). Low-swelling chitosan derivatives as biosorbents for basic dyes. *Langmuir*, *24*(9), 4791-4799.

[4] Sztandera, K., Gorzkiewicz, M., & Klajnert-Maculewicz, B. (**2018**). Gold nanoparticles in cancer treatment. *Molecular pharmaceutics*, *16*(1), 1-23..

[5] Huang, X., & El-Sayed, M. A. (**2010**). Gold nanoparticles: Optical properties and implementations in cancer diagnosis and photothermal therapy. *Journal of advanced research*, *1*(1), 13-28.

[6] Xia, Y., Xiong, Y., Lim, B., & Skrabalak, S. E. (**2009**). Shape-controlled synthesis of metal nanocrystals: simple chemistry meets complex physics?. *Angewandte Chemie International Edition*, *48*(1), 60-103.

[7] Liang, A., Liu, Q., Wen, G., & Jiang, Z. (**2012**). The surface-plasmon-resonance effect of nanogold/silver and its analytical applications. *TrAC Trends in Analytical Chemistry*, *37*, 32-47.

[8] Toderas, F., Baia, M., Maniu, D., & Astilean, S. (**2008**). Tuning the plasmon resonances of gold nanoparticles by controlling their size and shape. *Journal of optoelectronics and advanced materials*, *10*(9), 2282-2284.

[9] Link, S., & El-Sayed, M. A. (**2003**). Optical properties and ultrafast dynamics of metallic nanocrystals. *Annual review of physical chemistry*, *54*(1), 331-366.

[10] Huang, X., Jain, P. K., El-Sayed, I. H., & El-Sayed, M. A. (**2007**). Gold nanoparticles: interesting optical properties and recent applications in cancer diagnostics and therapy, 681−693.

[11] Murphy, C. J., Gole, A. M., Hunyadi, S. E., Stone, J. W., Sisco, P. N., Alkilany, A., ... & Hankins, P. (**2008**). Chemical sensing and imaging with metallic nanorods. *Chemical Communications*, (5), 544-557..

[12] Dulkeith, E., Ringler, M., Klar, T. A., Feldmann, J., Munoz Javier, A., & Parak, W. J. (**2005**). Gold nanoparticles quench fluorescence by phase induced radiative rate suppression. *Nano letters*, *5*(4), 585-589.

[13] Anger, P., Bharadwaj, P., & Novotny, L. (**2006**). Enhancement and quenching of single-molecule fluorescence. *Physical review letters*, *96*(11), 113002.

[14] Sapsford, K. E., Berti, L., & Medintz, I. L. (**2006**). Materials for fluorescence resonance energy transfer analysis: beyond traditional donor–acceptor combinations. *Angewandte Chemie International Edition*, *45*(28), 4562-4589..

[15] Xue, C., Kung, C. C., Gao, M., Liu, C. C., Dai, L., Urbas, A., & Li, Q. (**2015**). Facile fabrication of 3D layer-by-layer graphene-gold nanorod hybrid architecture for hydrogen peroxide based electrochemical biosensor. *Sensing and Bio-Sensing Research*, *3*, 7-11.

[16] Same, S., Aghanejad, A., Nakhjavani, S. A., Barar, J., & Omidi, Y. (**2016**). Radiolabeled theranostics: magnetic and gold nanoparticles. *BioImpacts: BI*, *6*(3), 169.

[17] El-Sayed, M. A. (**2001**). Some interesting properties of metals confined in time and nanometer space of different shapes. *Accounts of chemical research*, *34*(4), 257-264.

[18] Masters, A., & Bown, S. G. (**1992**, July). Interstitial laser hyperthermia. In *Seminars in surgical oncology* (Vol. 8, No. 4, pp. 242-249). New York: John Wiley & Sons, Inc.

[19] Shanmugam, V., Selvakumar, S., & Yeh, C. S. (**2014**). Near-infrared light-responsive nanomaterials in cancer therapeutics. *Chemical Society Reviews*, *43*(17), 6254-6287..

[20] Hong, E. J., Choi, D. G., & Shim, M. S. (**2016**). Targeted and effective photodynamic therapy for cancer using functionalized nanomaterials. *Acta Pharmaceutica Sinica B*, *6*(4), 297-307.

[21] Link, S., & El-Sayed, M. A. (**2000**). Shape and size dependence of radiative, non-radiative and photothermal properties of gold nanocrystals. *International reviews in physical chemistry*, *19*(3), 409-453..

[22] Harris, N., Ford, M. J., & Cortie, M. B. (**2006**). Optimization of plasmonic heating by gold

nanospheres and nanoshells. *The Journal of Physical Chemistry B*, *110*(22), 10701-10707.

[23] Khlebtsov, B. N., Khanadeev, V. A., Maksimova, I. L., Terentyuk, G. S., & Khlebtsov, N. G. (**2010**). Silver nanocubes and gold nanocages: fabrication and optical and photothermal properties. *Nanotechnologies in Russia*, *5*(7-8), 454-468.

[24] Link, S., & El-Sayed, M. A. (**1999**). Spectral properties and relaxation dynamics of surface plasmon electronic oscillations in gold and silver nanodots and nanorods, 8410−8426.

[25] Murphy, C. J., Sau, T. K., Gole, A. M., Orendorff, C. J., Gao, J., Gou, L., ... & Li, T. (**2005**). Anisotropic metal nanoparticles: synthesis, assembly, and optical applications, *109*, 13857−13870.

[26] Loo, C., Lin, A., Hirsch, L., Lee, M. H., Barton, J., Halas, N., ... & Drezek, R. (**2004**). Nanoshell-enabled photonics-based imaging and therapy of cancer. *Technology in cancer research & treatment*, *3*(1), 33-40..

[27] Terentyuk, G. S., Maslyakova, G. N., Suleymanova, L. V., Khlebtsov, N. G., Khlebtsov, B. N., Akchurin, G. G., ... & Tuchin, V. V. (**2009**). Laser-induced tissue hyperthermia mediated by gold nanoparticles: toward cancer phototherapy. *Journal of biomedical optics*, *14*(2), 021016.

[28] Khlebtsov, B., Melnikov, A., Zharov, V., & Khlebtsov, N. (**2006**). Absorption and scattering of light by a dimer of metal nanospheres: comparison of dipole and multipole approaches. *Nanotechnology*, *17*(5), 1437.

[29] Lapotko, D., Lukianova, E., Potapnev, M., Aleinikova, O., & Oraevsky, A. (**2006**). Method of laser activated nano-thermolysis for elimination of tumor cells. *Cancer letters*, *239*(1), 36-45.

[30] Lapotko, D. O., Lukianova-Hleb, E. Y., & Oraevsky, A. A. (**2007**). Clusterization of nanoparticles during their interaction with living cells, 241−253.

[31] Ghosh, P., Han, G., De, M., Kim, C. K., & Rotello, V. M. (**2008**). Gold nanoparticles in delivery applications. *Advanced drug delivery reviews*, *60*(11), 1307-1315.

[32] Alba-Molina, D., Martín-Romero, M. T., Camacho, L., & Giner-Casares, J. J. (**2017**). Ion-Mediated Aggregation of Gold Nanoparticles for Light-Induced Heating. *Applied Sciences*, *7*(9), 916.

[33] Yslas, E. I., Ibarra, L. E., Molina, M. A., Rivarola, C., Barbero, C. A., Bertuzzi, M. L., & Rivarola, V. A. (**2015**). Polyaniline nanoparticles for near-infrared photothermal destruction of cancer cells. *Journal of Nanoparticle Research*, *17*(10), 389.

[34] An, Z., & Yamaguchi, M. (**2012**). Chiral recognition in aggregation of gold nanoparticles grafted with helicenes. *Chemical Communications*, *48*(59), 7383-7385.

[35] Liu, C. W., Hsieh, Y. T., Huang, C. C., Lin, Z. H., & Chang, H. T. (**2008**). Detection of mercury (II) based on Hg 2+–DNA complexes inducing the aggregation of gold nanoparticles. *Chemical Communications*, (19), 2242-2244..

[36] Ma, Y., & Yung, L. Y. L. (**2014**). Detection of dissolved CO2 based on the aggregation of gold nanoparticles. *Analytical chemistry*, *86*(5), 2429-2435.

[37] Dansby-Sparks, R. N., Jin, J., Mechery, S. J., Sampathkumaran, U., Owen, T. W., Yu, B. D., ... & Xue, Z. L. (**2010**). Fluorescent-dye-doped sol− gel sensor for highly sensitive carbon dioxide gas detection below atmospheric concentrations. *Analytical chemistry*, *82*(2), 593-600..

[38] Koch, G. J., Beyon, J. Y., Gibert, F., Barnes, B. W., Ismail, S., Petros, M., ... & Singh, U. N. (**2008**). Side-line tunable laser transmitter for differential absorption lidar measurements of CO 2: design and application to atmospheric measurements. *Applied optics*, *47*(7), 944-956..

[39] Walt, D. R., Gabor, G., & Goyet, C. (**1993**). Multiple-indicator fiber-optic sensor for high-resolution pCO2 sea water measurements. *Analytica chimica acta*, *274*(1), 47-52.

[40] Cole, J. J., Caraco, N. F., Kling, G. W., & Kratz, T. K. (**1994**). Carbon dioxide supersaturation in the surface waters of lakes. *Science*, *265*(5178), 1568-1570.

[41] De Gregorio, S., Camarda, M., Longo, M., Cappuzzo, S., Giudice, G., & Gurrieri, S. (**2011**). Long-term continuous monitoring of the dissolved CO2 performed by using a new device in groundwater of the Mt. Etna (southern Italy). *Water research*, *45*(9), 3005-3011.

[42] Hanstein, S., de Beer, D., & Felle, H. H. (**2001**). Miniaturised carbon dioxide sensor designed for measurements within plant leaves. *Sensors and Actuators B: Chemical*, *81*(1), 107-114.

[43] Descoins, C., Mathlouthi, M., Le Moual, M., & Hennequin, J. (**2006**). Carbonation monitoring of beverage in a laboratory scale unit with on-line measurement of dissolved CO2. *Food Chemistry*, *95*(4), 541-553.

[44] Frahm, B., Blank, H. C., Cornand, P., Oelßner, W., Guth, U., Lane, P., ... & Pörtner, R. (**2002**). Determination of dissolved CO2 concentration and CO2 production rate of mammalian cell suspension culture based on off-gas measurement. *Journal of biotechnology*, *99*(2), 133-148.

[45] Mills, A., Lepre, A., & Wild, L. (**1997**). Breath-by-breath measurement of carbon dioxide using a plastic film optical sensor. *Sensors and Actuators B: Chemical*, *39*(1-3), 419-425..

[46] Jin, W., Jiang, J., Song, Y., & Bai, C. (**2012**). Real-time monitoring of blood carbon dioxide tension by fluorosensor. *Respiratory physiology & neurobiology*, *180*(1), 141-146.

[47] Mafuné, F., Kohno, J. Y., Takeda, Y., & Kondow, T. (**2001**). Dissociation and aggregation of gold nanoparticles under laser irradiation. *The Journal of Physical Chemistry B*, *105*(38), 9050-9056..

[48] Nam, J., Won, N., Jin, H., Chung, H., & Kim, S. (**2009**). pH-induced aggregation of gold nanoparticles for photothermal cancer therapy. *Journal of the American Chemical Society*, *131*(38), 13639-13645.

[49] Sato, K., Hosokawa, K., & Maeda, M. (**2003**). Rapid aggregation of gold nanoparticles induced by non-cross-linking DNA hybridization. *Journal of the American Chemical Society*, *125*(27), 8102-8103..

[50] Scarpettini, A. F., & Bragas, A. V. (**2010**). Coverage and aggregation of gold nanoparticles on silanized glasses. *Langmuir*, *26*(20), 15948-15953..

[52] Shamsipur, M., Safavi, A., Mohammadpour, Z., & Ahmadi, R. (**2016**). Highly selective aggregation assay for visual detection of mercury ion based on competitive binding of sulfur-doped carbon nanodots to gold nanoparticles and mercury ions. *Microchimica Acta*, *183*(7), 2327-2335..

[53] Thanh, N. T. K., & Rosenzweig, Z. (**2002**). Development of an aggregation-based immunoassay for anti-protein A using gold nanoparticles. *Analytical chemistry*, *74*(7), 1624-1628.

[54] Wu, Y., Zhan, S., Wang, F., He, L., Zhi, W., & Zhou, P. (**2012**). Cationic polymers and aptamers mediated aggregation of gold nanoparticles for the colorimetric detection of arsenic (III) in aqueous solution. *Chemical communications*, *48*(37), 4459-4461.

[55] Keshvari, F., Bahram, M., & Farhadi, K. (**2016**). Sensitive and selective colorimetric sensing of acetone based on gold nanoparticles capped with l-cysteine. *Journal of the Iranian Chemical Society*, *13*(8), 1411-1416..

[56] Pournaghi, A., Keshvari, F., & Bahram, M. (**2019**). Colorimetric determination of iodine based on highly selective and sensitive anti-aggregation assay. *Journal of the Iranian Chemical Society*, *16*(1), 143-149.

[57] Keshvari, F., Bahram, M., & Farshid, A. A. (**2015**). Gold nanoparticles biofunctionalized (grafted) with chiral amino acids: a practical approach to determining the enantiomeric percentage of racemic mixtures. *Analytical Methods*, *7*(11), 4560-4567..

[58] Mohseni, N., & Bahram, M. (**2018**). Highly selective and sensitive determination of dopamine in biological samples via tuning the particle size of label-free gold nanoparticles. *Spectrochimica Acta Part A: Molecular and Biomolecular Spectroscopy*, *193*, 451-457..

[59] Mohseni, N., Bahram, M., & Baheri, T. (**2017**). Chemical nose for discrimination of opioids based on unmodified gold nanoparticles. *Sensors and Actuators B: Chemical*, *250*, 509-517.

[60] Bahram, M., Alizadeh, S., & Madrakian, T. (**2015**). Application of silver nanoparticles for simple and rapid spectrophotometric determination of acetaminophen and gentamicin in real samples. *Sensor Letters*, *13*, 1-7.

[61] Bahram, M., Alizadeh, S., & Madrakian, T. (**2017**). Highly Selective and Sensitive Simultaneous Determination of Hemoglobin and Folic Acid Based on the Aggregation of PHCA Modified-Gold Nanoparticles Using Partial Least Square. *Sensor Letters*, *15*, 1-10.

[62] Alizadeh, S. (**2018**). Simple and rapid Simultaneously Colorimetric determination of betamethasone and nephazoline based on partial least square using gold nanoparticle probe. *Int J Bio-tech & Bioeng*, *4*, 1-17.

[63] Bahram, M., Madrakian, T., & Alizadeh, S. (**2017**). Simultaneous colorimetric determination of morphine and ibuprofen based on the aggregation of gold nanoparticles using partial least square. *Journal of pharmaceutical analysis*, *7*(6), 411-416.

[64] Alizadeh, S., Moghtader, M., & Aliasgharlou, N. (**2019**). Rank Annihilation Factor Analysis for Spectrophotometric Study of Morphine Based on Gold Nanoparticle Aggregation Using Multivariate Curve Resolution. *Sensor Letters*, *17*, 1-7.

How to cite this manuscript: Sakineh Alizadeh, Zahra Nazari, A Review on Gold Nanoparticles Aggregation and Its Applications, *Journal of Chemical Reviews*, **2020**, 2(4), 228-242.